Observations of Oscillating Cavitation on a Flat Plate Hydrofoil

Kotaro SATO
Kogakuin University, Shinjyuku, Tokyo, JAPAN
Masayuki TANADA
Toyota Motor Corporation, Toyota, Aichi, JAPAN
Sachie MONDEN
Mitsubishi Electric Corporation, Amagasaki, Hyogo, JAPAN
Yoshinobu TSUJIMOTO
Osaka University, Toyonaka, Osaka, JAPAN

Abstract

An experimental investigation was made to clarify the characteristics of oscillating cavitation on a flat plate hydrofoil in a water tunnel. Dynamic behavior of oscillating cavitation is discussed from the unsteady pressure measurements at the upstream of the blade and the visual observations of cavitation phenomena using high-speed video recording. It was found that the mean cavity length characterizes the fundamental characteristics of cavity oscillation. The cavity oscillations are categorized into two types, i.e. the transitional cavity oscillation and the partial cavity oscillation.

1. Intoroduction

If the cavity length of partial cavitation on a hydrofoil extends beyond 75 % of chord length, oscillating cavitation with change of cavity volume occurs. This kind of oscillating cavitation has been recognized as a transitional process between the partial cavitation and supercavitation, standing on theoretical results obtained by steady-linear analysis of Geurst (1959, 1960). This is herein called “transitional cavity oscillation”. This transitional cavity oscillation brought to attention by Wade and Acosta in 1966 has been studied by many researchers such as Kamono et al.(1992), Kuwako et al.(1993) and Matsudaira et al.(1995). However, these investigations were the only fragmentary examples, leaving the systematic understanding of oscillating characteristics to be clarified.

On the other hand, for the case of cavity length less than 75 % chord, another type of cavity oscillation has been observed by Kubota et al.(1986), Kamono et al.(1992), Le et al.(1992) and Kawanami et al.(1998). In the present paper, we call it “the partial cavity oscillation”. It is reported by Tanimura et al.(1995) that the oscillating partial cavity forms a re-entrant jet during its collapse, followed by a release of vortex cavity toward the downstream periodically. However, only few attempts have been made to date to clarify the similarity or difference of the oscillating

characteristic, between the transitional cavity oscillation and the partial cavity oscillation.

For the understanding of the phenomena, it is important to distinguish between the local flow instability around hydrofoil and the system instability, which is often associated with the change of total cavity volume. In traditional investigations, the cavitation number σ is recognized as one of the most important parameters to characterize the steady or unsteady cavitation phenomena. In the case of cavitation on a hydrofoil, the angle of attack α is also an important parameter. It is wall-known that the steady cavity length is determined by σ/2α based on the linear analysis. Recently, Watanabe et al.(1998) have shown theoretically that the characteristics of unsteady cavitation depends on the value of σ/2α. Kjeldsen et al.(1998), Pham et al. (1998) attempted to correlate the experimental results on unsteady cavitation with σ/2α.

In the present study, we attempt to categorize the above mentioned oscillating cavitations on a flat plate hydrofoil according to the non-dimensional cavity length based on the hydrofoil chord. The relationship between the characteristics of oscillation and type of cavitation (i.e. sheet cavitation and cloud cavitation) is discussed from the high-speed flow observations and fluctuating pressure measurements. The influence of the water tunnel system on the oscillating characteristics is also discussed. Furthermore, re-entrant jets were observed by means of dye injection and their effects on transitional cavity oscillation are discussed.

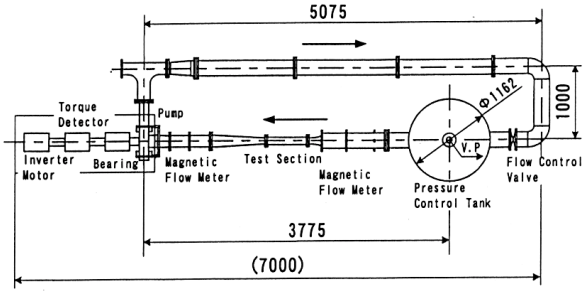

Fig. 1 Experimental apparatus.

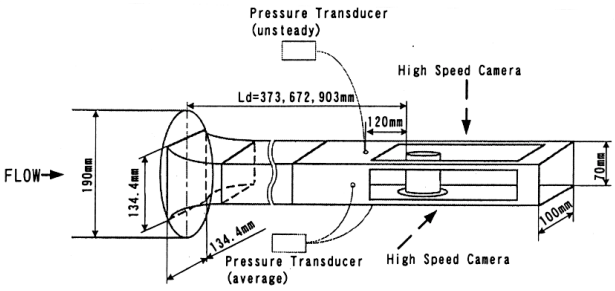

Fig. 2 Test section

(C=70[mm],Ld=373[mm],672[mm],903[mm])

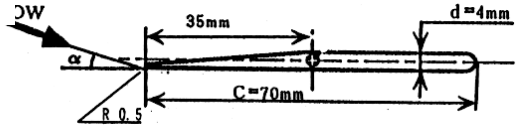

Fig. 3 Foil shape. (Chord C=70[mm], Span B=70[mm])

2. Experimental Method

Experimental apparatus is shown in Figure 1. Tank volume is 2.2 [m^3] and 70-80 percent of the volume is filled with deairated tap water. A three bladed inducer is used as the recirculating pump at the flow rate coefficient of Φ=0.1 which is larger than the design flow coefficient of Φ=0.078. It was confirmed by preliminary experiments that the operating conditions is out of range of flow instability produced by the inducer pump system, such as rotating cavitation or surge throughout the present experiments. The experiment was carried out at the inlet pressure of p=12[kPa], and the cavitation number was controlled by changing the flow velocity in a range of U=2.0～4.5[m/s], by adjusting the rotational speed of the recirculating inducer pump. The effects of the difference of the Reynolds number on the fundamental characteristics of cavity oscillation were not identified. Figure 2 shows the test section of water tunnel. A nozzle with the cross section area ratio of 4.65 was placed upstream of the hydrofoil. The distance between the nozzle and hydrofoil was changed to examine the system dependence of the cavity oscillations. Flat plate hydrofoil with chord length 70[mm] and span 70[mm] was employed in present experiment. The shape of the hydrofoil is shown in Figure 3. The angle of attack is defined as the angle between main flow and suction surface (the side with flat surface) of the blade. Mean flow velocity and pressure fluctuation were measured by an electromagnetic flow meter and a pressure transducer, respectively. The behavior of cavity on the hydrofoil was observed by a high-speed video recording system (NAC HSV-500) with a strobe lighting system. Framing rate 250 [fps] was used. In the present paper, cavity length L is defined as distance from the leading edge to end of continuously distributed cavity which is estimated from the high-speed video picture.

3. Inlet Pressure Fluctuation

Figure 4 shows the power spectrums of the inlet pressure fluctuation for various normalized cavity length Lc*=Lc/C, where Lc is the mean cavity length, C the chord length. Figures 4 (a) and (b) are typical results at angle of attack α=1.5 [deg] and 5 [deg], respectively. Before discussing the characteristics of cavity oscillation, a few remarks should be made concerning the type of cavitation. Several examples of photographs will be shown in next section. When the angle of attack is α=1.5 [deg], sheet cavitation was observed for any cavity length. In the case of α=5 [deg], both sheet and cloud cavitation are observed for longer cavities but only cloud cavities are observed for shorter cavities. In the present paper, it is categorized as the sheet cavitation if it appears some part of the cavity. The characteristics of cavity oscillation are represented by the non-dimensional amplitude of the inlet pressure fluctuation Ap*, and the Strouhal number Stb based on the hydrofoil chord C. In both Figures 4 (a) and (b), the frequency components caused by the transitional cavity oscillation can be seen at Stb=0.13 under the condition that non-dimensional cavity length Lc* is around unity (cf. (1) or (2) in Fig.4 (a) and (b)). It will be shown in the next

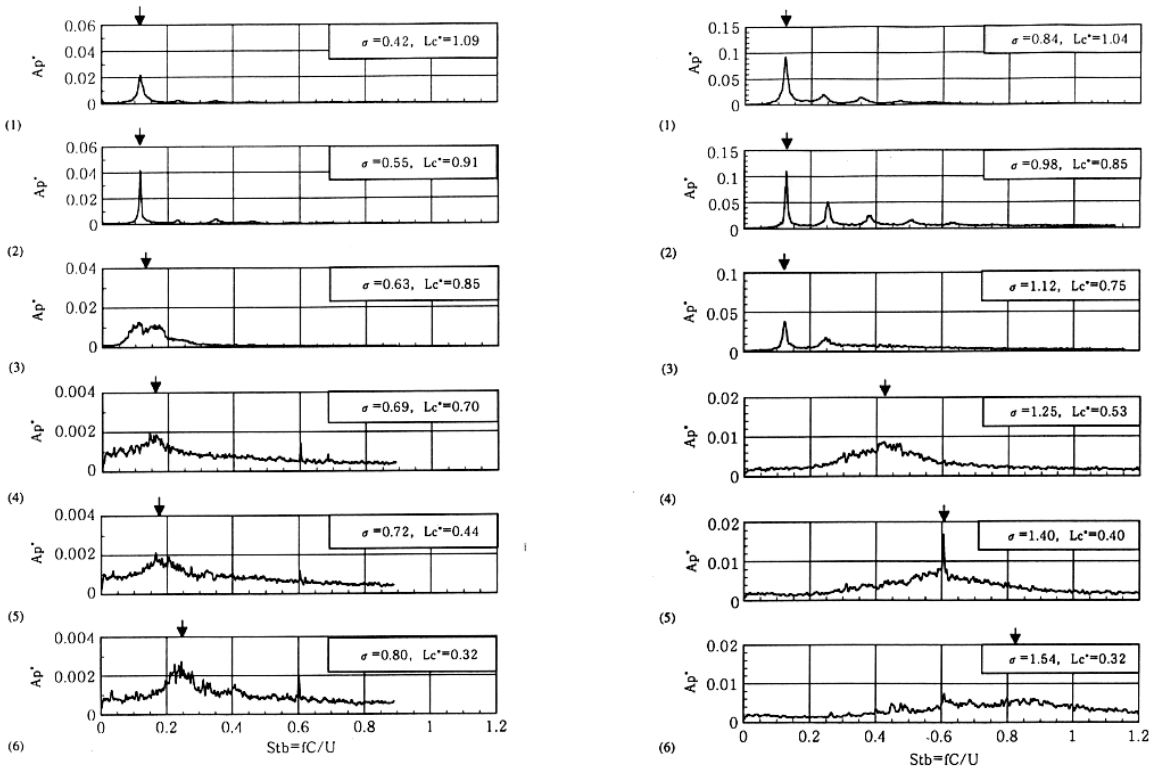

(a) α =1.5[deg], σ =0.42~0.80, Ld=373[mm] (b) α =5[deg], σ =0.84~1.54, Ld=373[mm]

Fig. 4 Power spectrums of inlet pressure fluctuation.

section that the frequency of inlet pressure fluctuation agrees with the frequency of cavity length oscillation. On the other hand, in spectrums (4) - (6), the pressure fluctuation with broadband frequency caused by the partial cavity oscillation can be observed for shorter cavities. The peak frequency shown by the arrows are considered as the representative frequency and is used in the following discussions. We notice that the magnitude at the peak increases with increasing non-dimensional cavity length Lc*. Furthermore, Strouhal number Stb for α=1.5 [deg] is smaller than that for α=5 [deg]. In the case of the transitional cavity oscillation, we cannot identify the fundamental difference between α=1.5 [deg] and 5 [deg] from (1) and (2). Thus the Strouhal number for the transitional cavity oscillation is independence of angle of attack.

In Figures 5 and 6, the relations between the non-dimensional cavity length Lc* and Strouhal number measured with various distance between the nozzle and hydrofoil are shown to examine the effect of the system on the characteristics of cavity oscillation. Figure 5 is for α=1.5 [deg] and Figure 6 α=5 [deg] where (a) shows Strouhal number Stb based on chord length and (b) represents Stc based on mean cavity length. In Figure 6, experimental data by other researchers are also plotted to compare with the present result. Figure 5 (a) and Figure 6 (a) show that the Strouhal number Stb is nearly constant over 0.75<Lc*<1.2 and independent on the angle of attack and inlet conduit length including the data by other researchers. Therefore we can say that Stb of transitional cavity oscillation is not largely affected by the cavity length, angle of attack, shape of hydrofoil and

experimental equipment system. Let us consider the partial cavity oscillation. For the partial cavity oscillation with Lc*<0.75, Strouhal number Stb based on the chord length increases with decreasing non-dimensional cavity length Lc*. For α=5 [deg] (see Figure 6(a)), with cloud cavitation, Stb for identical Lc* decreases approximately in inverse proportion to $\sqrt{Ld}$ where Ld is the distance from the nozzle to the leading edge of hydrofoil. This tendency is in agreement with an analytical result obtained by a 1-D flow model, which assumes that the pressure fluctuation near the leading edge is caused by the inertia of the fluid in the inlet conduit, associated with the cavity volume change. For α=5 [deg], the effect of Ld/C is not evident. The difference between α=5 [deg] and α=1.5 [deg] may be associated with the difference of type of cavitation cloud type for α=5 [deg] and sheet type for α=1.5 [deg].

Figure 5 (b) and Figure 6 (b) show the relation between non-dimensional cavity length Lc* and Strouhal number Stc based on cavity length. In the case of sheet cavitation (all data in Figure 5 (b) and for the data with 0.75<Lc* in Figure 6 (b)), Stc distributes in a narrow range between 0.1 and 0.2. However Stc for the partial cavity oscillation with cloud cavitation (0<Lc*<0.75 in Figure 6

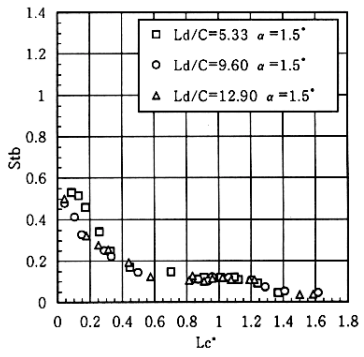

(a) Strouhal number Stb=fC/U

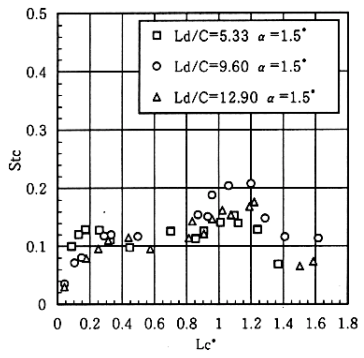

(b) Strouhal number Stc=fLc/U

Fig. 5 Relation between cavity length and Sttrohal number obtained by inlet pressure fluctuation for smaller angle of attack.

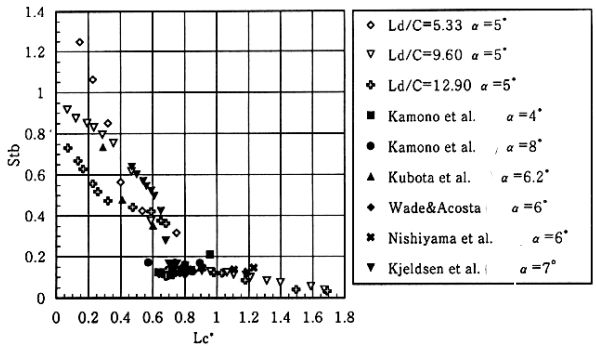

(a) Strouhal number Stb=fC/U

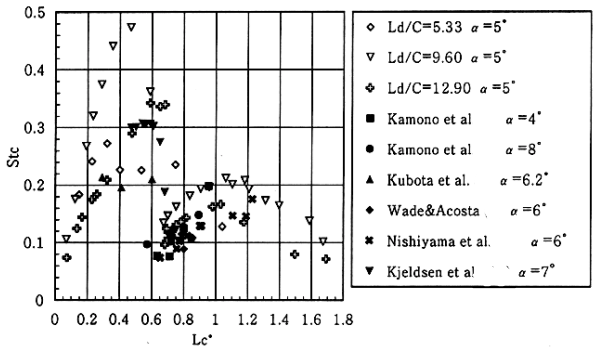

(b) Strouhal number Stc=fLc/U

Fig. 6 Relation between cavity length and Sttrohal number obtained by inlet pressure fluctuation for larger angle of attack.

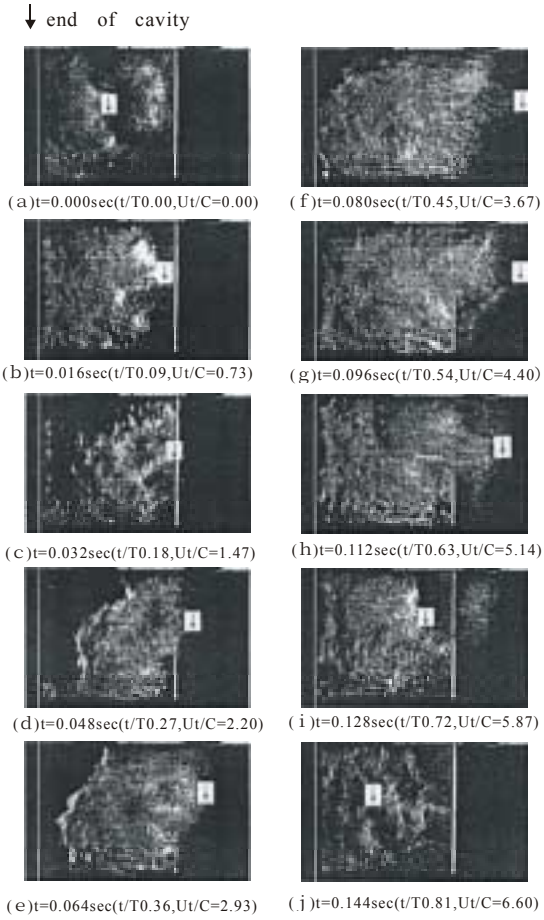

Fig. 7 Pictures of transitional cavity oscillation.

(α =5[deg], σ =0.77, C=70[mm], U=3.21[m/s], Ld=373[mm], Lc* 1.0)

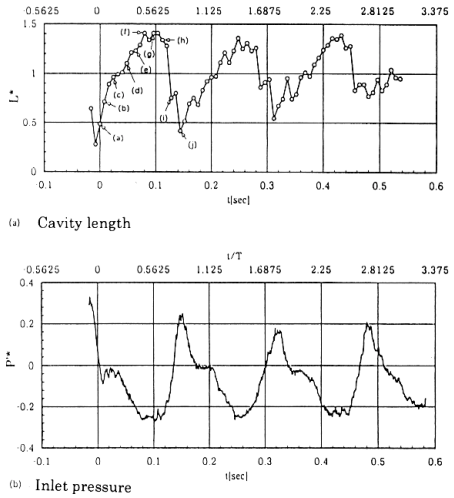

Fig. 8 Change of cavity length and inlet pressure with time in case of transitional cavity oscillation.

(α =5[deg], σ =0.77, C=70[mm], U=3.21[m/s], Ld=373[mm])

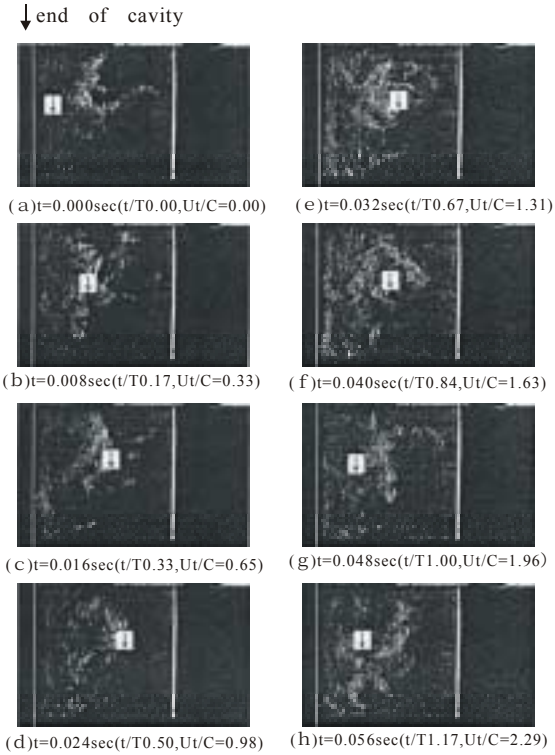

Fig. 9 Pictures of transitional cavity oscillation.

(α =5[deg], σ =1.18, C=70[mm], U=2.86[m/s], Ld=373[mm], Lc* 0.5)

(b)) depends significantly on the inlet conduit length. In the present experiment, it is noticed that values of Stc for cloud cavitation are generally greater than that for sheet cavitation. Similar results as shown in Figures 5 and 6 have been obtained by Kjeldsen et al.(2000) for a NACA 0015 hydrofoil. Major difference is that they observed more distinct partial cavity oscillations with discrete spectrum. However, it would be more important to note the fact that the two types of cavity oscillations are observed with completely different hydrofoil shapes and in different systems.

4. Photographic Observation

Photographs of the transitional cavity oscillation for α=5 [deg], Lc*=1 are shown in Figure 7. The arrows in the figures indicate the cavity trailing edge in each frame. In this figure, the period of cavity oscillation agrees with the period of oscillation determined from the inlet pressure fluctuation. We can observe the growth phase of cavity in (a) - (f) and the collapse phase in (f) – (j). It can be seen that the sheet cavitation appears near the leading edge in (d) and (e), but it changes to cloud cavitation shortly and is separated from the main cavity and shed downstream in (h) and (i). In this condition, the frequency of the cloud cavity shedding is equivalent to the frequency of cavity length change with time. Figure8 shows the change of cavity length and inlet pressure with time for transitional cavity oscillation. (a) is cavity length and (b) inlet pressure change. In Figure 8 (a), (a) to (j) in the figure shows the instant of time corresponding to Figure 7 (a) to (j). Non-dimensional pressure fluctuation is defined as $P'^*=P'/(\rho U^2/2)$ where ρ is the density and P' is pressure fluctuation component. We notice that the phase of the cavity length fluctuation differs by π as compared with that of inlet pressure fluctuation. From this figure or Figure 4, it is also seen that the period of transitional cavity oscillation is almost identical for each cycle.

Figure 9 shows typical pictures of the partial cavity oscillation for α=5 [deg], Lc*=0.5. Since cloud cavitation starts from leading edge of hydrofoil in this situation, the pictures are not clear. Cloud cavity is shed in the collapse phase of the cavity on the blade. Figure10 shows the cavity length and inlet pressure change corresponding to the pictures shown in Figure 9. It is seen that the period of oscillation changes significantly for each cycle as compared with the transitional cavity oscillation. This is the reason for the broadband spectrum of inlet pressure fluctuation. This figure shows that the cavity oscillation correlates with the inlet pressure fluctuation even in the case of partial cavity oscillation with broadband spectrum and smaller magnitude. Therefore, the inlet pressure fluctuation measurement is appropriate to evaluate the characteristics of both the transitional cavity oscillation and the partial cavity oscillation. The behavior of the partial cavity oscillation with sheet cavitation for α=1.5 [deg], Lc*=0.5 is shown in Figure 11. We can recognize the re-entrant jet toward leading edge of hydrofoil in (d) and (e).

5. Observation of Re-enrant Jet

Tanimura et al.(1995) introduced three proposed mechanisms to explain cavity oscillations, i.e. re-entrant jet, surface wave and impinging jet. They attempted to control the re-entrant jet by a bar attached on hydrofoil experimentally. It is reported that the pressure fluctuation resulting from the partial cavity oscillation is suppressed by the bar. However no studies have ever been made to explain the relation between the transitional cavity oscillation and

re-entrant jet. We present the observation of re-entrant jet on hydrofoil by means of dye injection for the case of transitional cavity oscillation to discuss about the effect of a bar on the characteristics of oscillating cavitation. The bar which has square cross section 3[mm]×3[mm] is attached at 1/3C from leading edge. Figure 12 is the behavior of the re-entrant jet on a hydrofoil without a bar and Figure 13 is for the case of hydrofoil with a bar. We can observe the region colored by the dye injected near the trailing edge migrate toward upstream in these figures. This shows that the re-entrant jet appears also for the transitional cavity oscillation at the collapse phase of cavity. Without a bar, as shown in Figure 12, dye reaches the leading edge. With a bar, as shown in Figure 13, the re-entrant jet is stopped by the bar. A cloud of cavity is shed after the re-entrant jet collides with the bar. Figure 14 (a) shows the typical observation of the cavity shed from the location of the bar. In Figure 14 (b), the locations of re-entrant jet and shed cavity are plotted against time. This figure clearly shows that the cloud of cavity is shed each time the re-entrant jet reaches the leading edge or the bar. However, the period of cavity shedding is not affected by the existence of the bar. Figure 15 and 16 are power spectrums of inlet pressure fluctuation for the case. with and without a bar. The spectrum in not substantially affected by the existence of the bar. These results lead to the conclusion that the transitional cavity oscillation is not controlled by the re-entrant jet and the associated cavity shedding although they do appear associated with the cavity oscillation. The present results suggest that the re-entrant appears as a result of transitional cavity oscillation rather

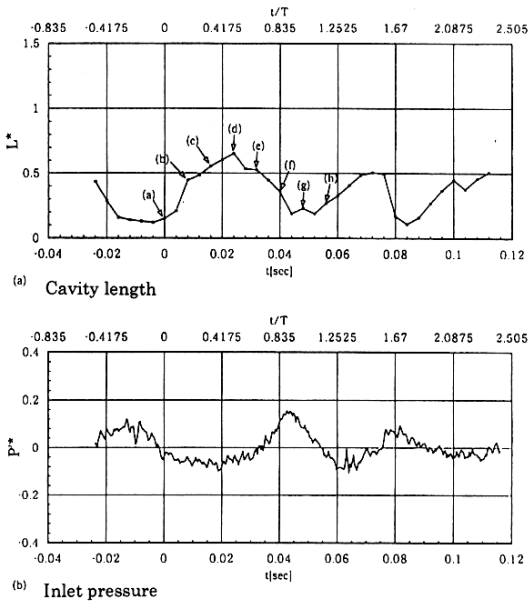

Fig. 10 Change of cavity length and inlet pressure with time in case of transitional cavity oscillation.
(α =5[deg], σ =1.18, C=70[mm], U=2.86[m/s], Ld=373[mm])

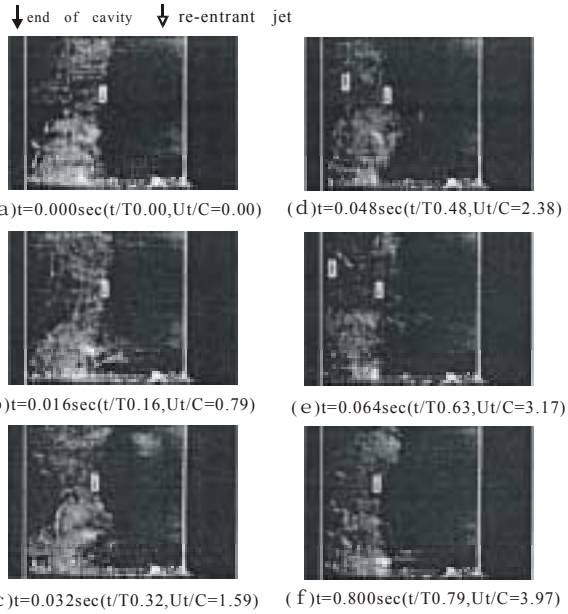

Fig. 11 Photographic observation of partial cavity oscillation. (α =1.5[deg], σ =0.68, C=70[mm], U=3.47[m/s], Ld=373[mm], Lc* 0.5)

than being the cause of it. By the way, Watanabe et al. (2000) shows that a linear time marching analysis using a closed cavity model without re-entrant jet can predict the frequencies of partial and transitional cavity oscillation.

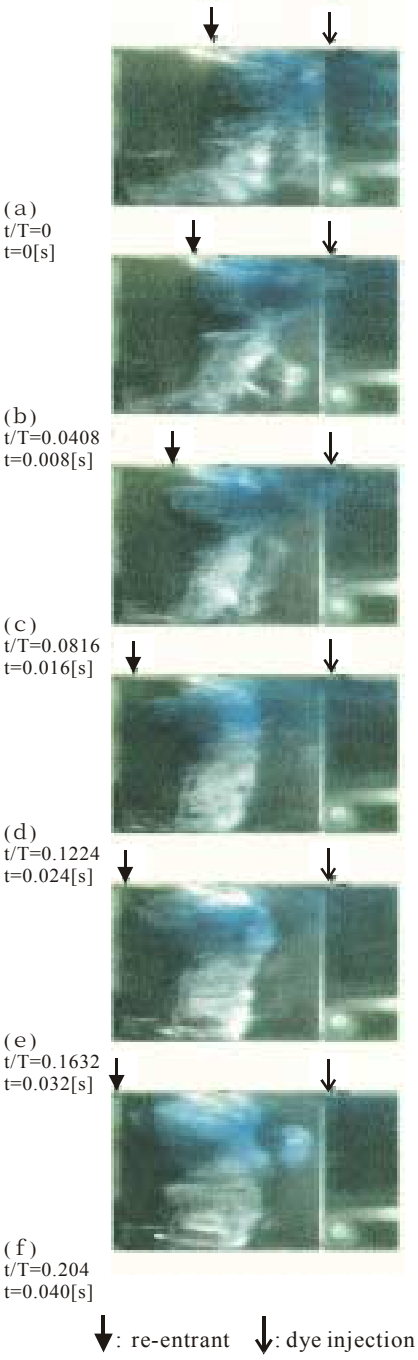

Fig. 12 Observation of re-entrant jet on foil without bar.
(α =3.8[deg], σ =0.88, U=3.50[m/s], Ld=373[mm], Lc* 1.0)

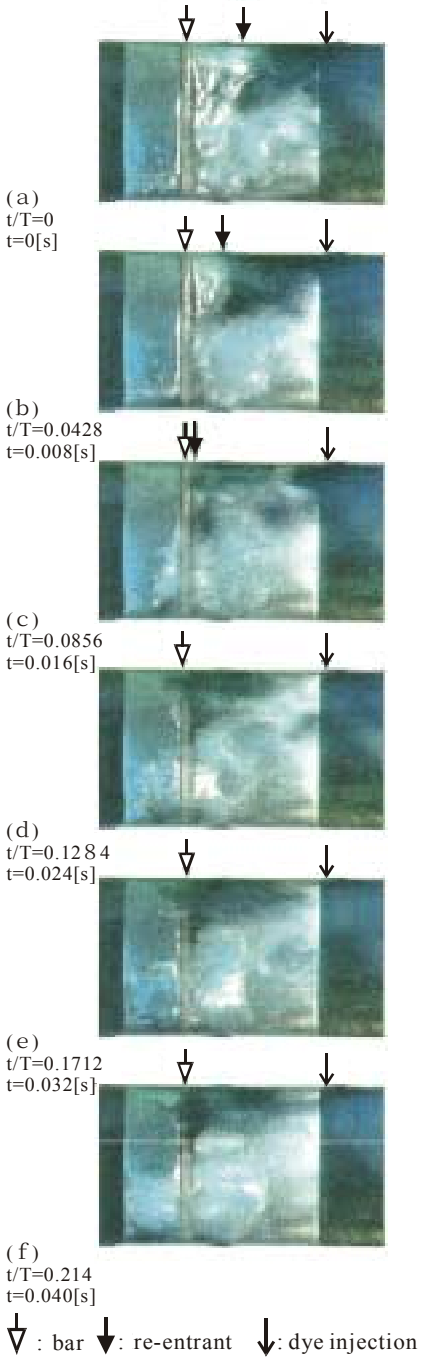

Fig. 13 Observation of re-entrant jet on foil without bar.
(α =3.8[deg], σ =0.80, U=3.59[m/s], Ld=373[mm], Lc* 1.0)

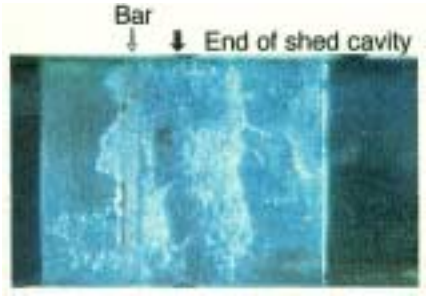

(a)

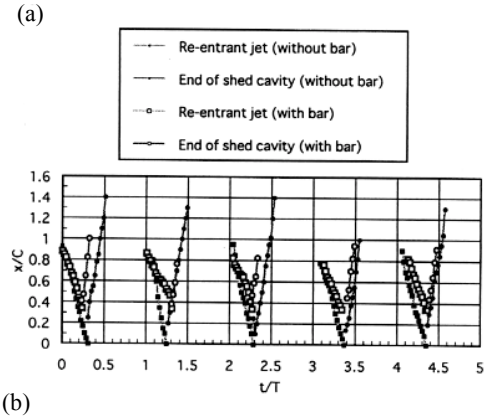

(b)

Fig. 14 Location of re-entrant jet and shed cavity.

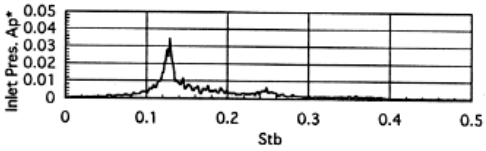

Fig. 15 Power spectrums of inlet pressure fluctuation in case of foil without bar.
(α =3.8[deg], σ =1.00, C=90[mm], U=3.50[m/s], Ld=373[mm], Lc* 1.0)

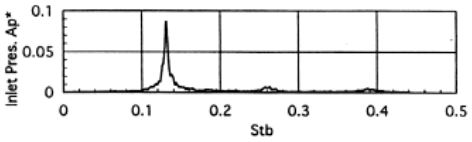

Fig. 16 Power spectrums of inlet pressure fluctuation in case of foil without bar.
(α =3.8[deg], σ =1.00, C=90[mm], U=3.59[m/s], Ld=373[mm], Lc* 1.0)

6. Conclution

An experimental study was made to clarify the characteristics of oscillating cavitation on a flat plate hydrofoil in a water tunnel. The following conclusions can be drawn.

(1) The oscillating cavitations can be grouped into two types: the transitional cavity oscillation and the partial cavity oscillation. They mainly depend on the mean cavity length. The transitional cavity oscillation occurs when non-dimensional cavity length is in range of 0.75<Lc*<1.2. For transitional cavity oscillations, the Strouhal number Stb Strouhal number Stb based on the chordlength of transitional cavity oscillation is nearly contant over the range of the cavity length (0.75<Lc*<1.2), and is not affected by the angle of attack, shape of hydrofoil and experimental system. For non-dimensional cavity length less than 0.75, partial cavity oscillation is observed. Strouhal number Stb of partial cavity oscillation increases with decreasing cavity length.

(2) When the angle of attack is small, sheet cavitation appears. In this situation, Strouhal number Stb does not largely depend on the inlet conduit length. On the other hand, cloud cavitation is observed under the condition with larger angle of attack. In the case of cloud cavitation, the Strouhal number Stb depends on the inlet conduit length.

(3) For the case of transitional cavity oscillations, re-entrant jet was observed using dye injection, with and without a bar on the foil to stop the re-entrant jet. It was found for both cases that the re-entrant jet is associated with cavity shedding. Even if we stop the reentrant jet by the bar, both frequency and the magnitude of oscillation did not change. From this observation, re-entrant jet is not the cause of transitional cavity oscillation but a result of cavity oscillation.

Acknowledgements

One of the authors (YT) would like to express sincere thanks for valuable discussions with Professors Rodger Arndt, Daniel Frumann and Jean-Pierre Franc. The authors wish to thank Dr Yoshiki Yoshida and Dr Satoshi Watanabe for their useful suggestions and Mr. Atsushi Hashimoto for his assistance in experiment.

References

Geurst, J. A. 1959 Linearized Theory for Partially Cavitated Hydrofoils. Int. shipbuilding Progress, Vol.6, No.60, pp.369-384

Geurst, J. A. 1960 Linearized Theory for Fully Catitated Hydrofoil. Int. shipbuilding Progress, Vol.7, No.65, pp.17-27

Kawanami, Y., Kato, H., and Yamaguchi, H. 1998 Three-dimensional Characteristics of the Cavities Formed on a Two-dimensional Hydrofoil. Proc. 3rd Int. Symp. Cav., pp.191-196

Kamono, H., Kato, H., Yamaguchi, H., Miyanaga, M and Ogawa, H. 1992 A Study of Ventilated Cavitation. 7th symposium on cavitation, pp.43-48 (in Japanese)

Kjeldsen, K., Effertz, M. and Arndt, R. 1998 Investigation of Unsteady Cavitation Phenomena. Proc. US-Japan Seminar : Abnormal Flow Phenomena in Turbo-machines, Osaka

Kjeldsen, M., Arndt, R. E. A. and Effertz, M. 1999 Investigation of Unsteady Cavitation Phenomena. Proceedings of the 3rd ASME/JSME Fluids Engineering Conference, San Francisco, CA, July

Kubota, A., Kato, H., Yamaguchi, H. and Maeda, M. 1986 Unsteady Structure of Cloud Cavitation on a Foil Section. Journal of the Society of Naval Architects of Japan. Vol.160, pp.78-92 (in Japanese)

Kuwako, H., Sakagami, K., Naka, H., Ito, Y. and Obe, R. 1993 Unsteady Behavior of Violent Vibralions Depending upon Type of Cavitation. JSME. Vol.59, No.559, pp.665-670 (in Japanese)

Le, Q., Franc, J. P. and Michel, J. M. 1993 Partial Cavities : Global Behaviour and Mean Pressure Distribution. ASME. J. of Fluids Eng. Vol.115, pp.243-248

Matsudaira, Y., Tamura, S., and Obara, H. 1995 Characteristics of a Cavitating Hydrofoil in Separation Region. JSME. Vol.61, No.592, pp.4271-4276 (in Japanese)

Nishiyama, T., Yoshioka, S. and Akama, M. 1983 Time Historical Analysis of Cavitation on Hydrofoil. JSME. Series B, Vol.49, No.448, pp.2655-2661 (in Japanese)

Pham, T. M., Larrarte, F. and Fruman, D.H. 1998 Investigation of Unstable Cloud Cavitation. Third International Symposium on Cavitation. Vol.1, pp.215-220

Tanimura, M., Tagaya, Y., Kato, H., Yamaguchi, H., Maeda, M. and Kawanami, Y. 1998 Mechanism of Clod Cavitation and Its Control. Journal of the Society of Naval Architects of Japan. Vol.178, pp.41-50 (in Japanese)

Wade, R. B. & Acosta, A. J. 1996 Experimental Observations on the Flow Past a Plane-Convex Hydrofoil. ASME. J. Basic Engineering, pp.273-283

Watanabe, S., Tsujimoto, Y., Franc, J-P., and Michel, J-M., 1998 Linear Analysis of Cavitation Instabilities, Proceedings of 3rd International Symposium on Cavitation, Vol.1, Grenoble, pp.347-352.

Watanabe, S., Tsujimoto, Y., and Furukawa, A., 2000, Theoretical analysis of Transitional and Partial Cavity Instabilities, Proceedings of ASME FEDSM'00, Boston, to be published in the Journal of Fluids Engineering.